Article

A first principles study of the energetics and core level shifts of anion-doped TiO₂ photocatalysts

Wuchen Ding, Weixue Li*

State Key Laboratory of Catalysis, Dalian Institute of Chemical Physics, Chinese Academy of Sciences, Dalian 110623, Liaoning, China

ARTICLE INFO

ABSTRACT

We present a comprehensive and improved density functional theory (DFT) calculation of anion-doped (anion = B, C, N, F, P, S) anatase and rutile TiO₂. The first part is a first principles calculation of the core level shifts (CLS) for various anion dopants in both anatase and rutile TiO₂. The CLS results revealed that interstitial N had a higher N 1s binding energy than substitutional N, which agreed well with experimental results. The calculation also showed that for B-, C-, S-, and P-doped TiO₂, the interstitial dopant had an energy that is higher than that of a substitutional dopant, which is similar to N-doped TiO₂. However, for F-doped TiO₂, the energy of the substitutional dopant is higher, and this is irrespective of the TiO₂ crystallography. We also calculated the enthalpy of doping and found that the substitutional dopant had a higher enthalpy than the interstitial dopant. The results revealed that substitutional doping required severe experimental conditions, whereas interstitial doping only requires modest wet chemistry conditions.

1. Introduction

In 1972, Fujishima et al. [1] discovered photoelectron chemical splitting of water on TiO₂ electrodes, which led to extensive investigations of TiO₂ as a photocatalyst. TiO₂ is one of the most promising photocatalysts for the photocatalytic degradation of organic pollutants and photocatalytic dissociation of water. However, the wide bandgap of anatase TiO₂ (3.2 eV) limits its photocatalytic applications to the ultraviolet (UV) light range. Meanwhile, the relatively high rate of electron-hole recombination results in a low quantum yield and poor efficiency in promoting photocatalytic reactions. These fundamental problems prevent the use of anatase TiO₂ in practical applications. Therefore, one of the endeavours to improve the performance of TiO₂ is to increase its optical efficiency by

shifting the onset of its response from the UV to the visible region [2–5]. One strategy is to dope TiO₂ with an anion such as B, C, N, F, P, or S to decrease its band gap.

Compared to other anion dopants, N has been proven to be one of the most efficient for visible light-responsive TiO₂ photocatalysts [3,5], and this system has been studied extensively by experiments. Various methods have been developed to prepare N-doped TiO₂ photocatalysts (powders and films), such as sputtering [3,6–8], ion implantation [9–12], controlled hydrolysis or sol-gel [13–24], and chemical treatment of TiO₂ [3,9,12,25–30]. Although these N-doped TiO₂ photocatalysts are visible light-active, there are debates on their structures, particularly on the location of the active N atoms and the origin of the bandgap narrowing in N-doped TiO₂. Asahi et al. [3] indicated that N atoms substituted for O atoms in N-doped TiO₂

---

and the decrease of the bandgap originated from the mixing of the O 2*p* and substitutional N 2*p* states. Diwald et al. [9] concluded that N atoms can also be located at interstitial sites in N-doped TiO₂, and they further confirmed that this nitrogen state was responsible for the observed shift of the photochemical threshold of rutile TiO₂(110) down to 2.4 eV. Irie et al. [12] proposed that the isolated narrow N 2*p* band formed by substitutional N in N-doped TiO₂ above the O 2*p* valence band was responsible for the visible light response. Serpone [31] argued that the visible light activation of N-doped TiO₂ was due to defects associated with oxygen vacancies that gave rise to color centers. Recently, Livraghi et al. [19] investigated N-doped TiO₂ by a combined experimental and theoretical approach and suggested that N_b• centers (single atom nitrogen in the bulk of TiO₂) played an essential role in the absorption of visible light, in the promotion of electrons to the conduction band, and in photoinduced electron transfer to reducible adsorbates. So far, the most common technique to detect doped N atoms in TiO₂ is by X-ray photoelectron spectroscopy (XPS). N 1*s* XPS peaks with different binding energies have been reported for N-doped TiO₂ prepared by different methods, but their assignments are still not conclusive. Compared with N in TiN, the N 1*s* XPS feature with its binding energy at 397.0 eV is generally assigned to N^{2-} anions that are substituted for O in the TiO₂ lattice. However, Chen et al. [32] attributed a N 1*s* peak with its binding energy at 401.3 eV to substitutional N in O–Ti–N. Diwald et al. [9] prepared N-doped rutile TiO₂(110) by heating in NH₃ and observed two N 1*s* peaks with binding energy at 396.7 and 399.6 eV, which were assigned to substitutional and interstitial N atoms, respectively. Rodriguez et al. [33] reported the N 1*s* binding energy of atomic N adsorbed on rutile TiO₂(110) to be 399.0 eV. Therefore, a clear understanding of the structures of N-doped TiO₂ photocatalysts is of great importance. Recently, other nonmetal-doped TiO₂ with dopants like B, C, or F have also received growing interest from both experiments and theoretical calculations [19,34–46].

In theoretical studies, Di Valentin et al. [19,36,41–46] have published a number of papers on nonmetal-doping of TiO₂. In their work, they performed a lot of electronic state analysis on the localized states formed in the band gap of TiO₂. In addition, they also performed core level shift (CLS) studies for different doping positions. Their CLS value of different N locations in N-doped anatase TiO₂ is 1.6 eV with the initial state approximation. They also showed in their calculations that there existd a difference of 2.6 eV between interstitial B and substitutional B with initial state relaxation effects considered [36]. However, their CLS results may be more convincing if they had considered final state relaxation in their calculations.

The locations of anions and thermodynamic stability are two aspects of most concern to experimentalists. Therefore, in this work, we comprehensively studied the CLS and thermodynamic stability for different doping anions (B, C, N, F, P, and S), different doping types (substitutional and interstitial), and different TiO₂ phases (rutile and anatase). In the energetics calculations, especially with N-doping, we have considered the difference between the PBE functional and hybrid HSE06 functional.

In the first part of the work, we determined the optimized structures of the anion-doped TiO₂. Then in the second part, we employed standard and hybrid density function theory (DFT) calculations for an energetics study of anion-doped TiO₂. We study the thermodynamics in an effort to find the fundamental reason for the different N-doped TiO₂ types identified by the different preparation methods. Although there are less experimental studies than on N-doped TiO₂, some conclusions for the systems of B-, C-, F-, P-, or S-doped TiO₂ can be given. In the last part, DFT calculations with final state relaxation effects included were employed to provide comprehensive and precise insight into the CLS results of anion-doped TiO₂. In this part, we studied different doping locations, anions, and TiO₂ phases. We hope these CLS calculations help distinguish the close peaks in the XPS spectra.

2. Theoretical approaches and computational details

Spin-polarized total energy calculations were performed based on the all-electron projected augmented wave (PAW) method and DFT within the generalized gradient approximation (GGA-PBE) using a HSE06 hybrid functional as implemented in the Vienna Ab Initio Simulation 5.2 Package (VASP) [47–54]. A cutoff of 400 eV was used for the plane wave expansion. Throughout the present work, optimized equilibrium lattice constants (anatase TiO₂: *a* = 3.82 Å, *c* = 9.62 Å; rutile TiO₂: *a* = 4.66 Å, *c* = 2.97 Å), which agreed well with previous calculations [45] and experiments (anatase TiO₂: *a* = 3.78 Å, *c* = 9.52 Å; rutile TiO₂: *a* = 4.59 Å, *c* = 2.96 Å) [5], were used unless otherwise stated. To study anion doping in the TiO₂ bulk, one anion atom was included in the anatase (3×3×1) supercell with dimensions of 11.46 Å × 11.46 Å × 9.62 Å and rutile (2×2×3) supercell with dimension of 9.32 Å × 9.32 Å × 8.91 Å, which corresponded to the doping concentration of 1.4% and 2.1%, respectively. For the Brillouin zone integration, we employed a Monkhorst-Pack (2×2×4) and (4×4×4) Γ-centered k-point grid for the anatase (3×3×1) and rutile (2×2×3) supercell. All the ions in the super cell were relaxed until the residual force on each ion was less than 0.01 eV/Å.

CLS were calculated as the energy difference between the core level binding energy of the atom of interest (E^i_{cl}) and a reference atom (E^{ref}_{cl}), i.e., CLS = E^i_{cl} − E^{ref}_{cl}. The core level binding energy (E_{cl}) can be calculated in both the initial state and final state approximations. In the initial state approximation, E_{cl} is the negative eigenvalue ($-\varepsilon_c$) of the orbital from which the core electron has been excited, where $E_{cl} = -\varepsilon_c$, and ε_c refers to the Fermi level for the solid and vacuum for the gas. In the final state approximation, E_{cl} was calculated by the total energy difference between the two configurations, which were an excited configuration in which an electron was removed from a particular core state, $E_{tot}(n_c - 1)$ and the ground state configuration, $E_{tot}(n_c)$. Thus, $E_{cl} = E_{tot}(n_c - 1) - E_{tot}(n_c)$, in which the core-hole was assumed to remain localized in the excited atom.

In this work, for the final state calculation, a core electron was removed from the core by generating the corresponding core excited ionic PAW potential in the calculation, and the remaining core states were relaxed in the self-consistent calcu-

lation.

3. Results and discussion

3.1. Optimized structures of anion-doped TiO₂

In this work both anion substitution and interstitial doping were considered. As all the O atoms are in the same position, there is only one possibility for the anion substitution location. However, for the interstitial-doped anion, there are three possible equivalent positions in anatase TiO₂ and two possible positions in rutile TiO₂, as shown in Fig. 1. The optimized coordinate of the interstitial N atoms in each structure and the total energy of the optimized structure are summarized in Fig. 2. For interstitial N-doped anatase, the A3 type exhibited the lowest total energy, in agreement with the previous result [45]. For interstitial N-doped rutile, the R2 type is more stable. Therefore, the a_2 type and the R2 type were chosen as the models for the further theoretical investigations of interstitial N-doped anatase and rutile, respectively. Similar work was done on the other anion-doped TiO₂. The results are listed in Table 1. It can be seen that the location depended on the size of the atomic radius. Larger anions prefer the larger interspace. Compared with bulk TiO₂, the atoms surrounding the doped anion were slightly relaxed in the anion-doped TiO₂.
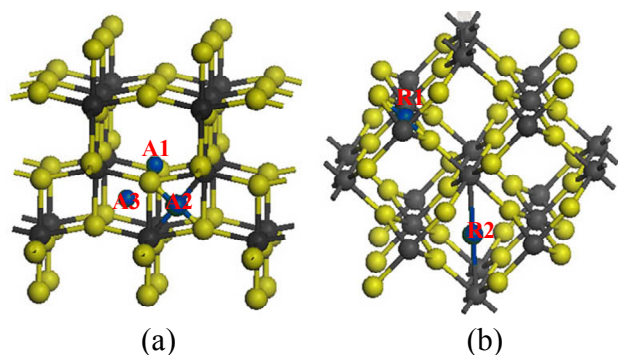

Fig. 1. Different interstitial sites in anatase TiO₂ (a) and rutile TiO₂ (b).
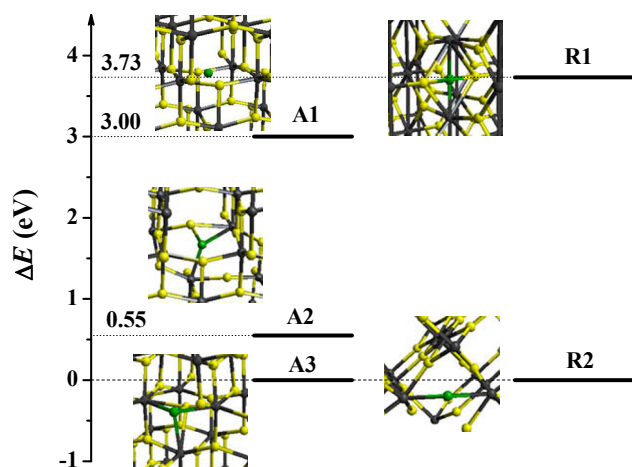

Fig. 2. Energy difference in N-doped TiO₂ after crystal relaxation.

Table 1

Interstitial doping anion sites used in the calculations and Pauli electronegativity of the atoms.
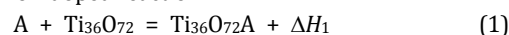
Atom	Anatase TiO₂	Rutile TiO₂	Atomic radius (pm) [55]	Pauli electronegativity [56]
B	A1[a]	R2	85	2.04
C	A2	R2	70	2.55
N	A2	R2	65	3.04
F	A2	R2	50	3.98
P	A1	R2	100	2.19
S	A2	R2	100	2.58
O		R2	60	3.44
Ti		R2	140	1.54

[a] Location of the anion (from Fig. 1).

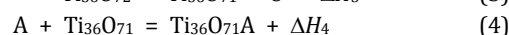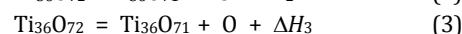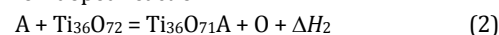### 3.2. Energetics study of anion-doped TiO₂

To compare the reaction enthalpy of the reactions producing interstitial and substitutional anion-doped TiO₂, we considered the reaction, which is that of one anion with TiO₂ to produce anion-doped TiO₂. The source of the anion atom would offset in the enthalpy comparison of two types of anion-doped TiO₂, thus for interstitial doping, there is only one process in which anions get into the favorable interstitial space of the TiO₂ lattice. However, for substitutional doping, there are three processes in which O atoms first are removed from the TiO₂ lattice leading to the formation of oxygen vacancies, and anions fill these vacancies at the same time. As the sources of the anion and final form of the O atom are not unique, the doping reaction can be described as the following for anatase TiO₂ on the basis of the structural model:
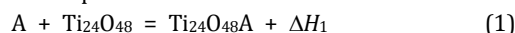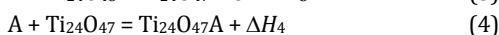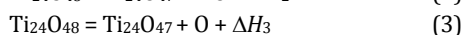
Interstitial anion-doped reaction

$$A + Ti_{36}O_{72} = Ti_{36}O_{72}A + \Delta H_1 \qquad (1)$$

Substituting anion-doped reaction

$$A + Ti_{36}O_{72} = Ti_{36}O_{71}A + O + \Delta H_2 \qquad (2)$$

$$Ti_{36}O_{72} = Ti_{36}O_{71} + O + \Delta H_3 \qquad (3)$$

$$A + Ti_{36}O_{71} = Ti_{36}O_{71}A + \Delta H_4 \qquad (4)$$

For rutile TiO₂, the doping reaction equations are the following:

Interstitial anion-doped reaction

$$A + Ti_{24}O_{48} = Ti_{24}O_{48}A + \Delta H_1 \qquad (1)$$

Substituting anion-doped reaction

$$A + Ti_{24}O_{48} = Ti_{24}O_{47}A + O + \Delta H_2 \qquad (2)$$

$$Ti_{24}O_{48} = Ti_{24}O_{47} + O + \Delta H_3 \qquad (3)$$

$$A + Ti_{24}O_{47} = Ti_{24}O_{47}A + \Delta H_4 \qquad (4)$$
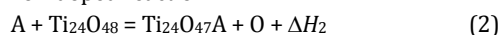
ΔH was calculated by the equation $\Delta H = \Sigma E(\text{products}) - \Sigma E(\text{reactants})$, in which E represents the total energy.

Reaction (2) is not the same as reaction (1), which has stable products, so the final form of the O atom should be included in reaction (2). In other words, there should be an additional enthalpy ΔH_5 added to ΔH_2 in the case of the comparison with ΔH_1, where ΔH_5 is the enthalpy of the process where the O atom changed into the final form, which is determined by the particular reaction route.

To identify the error from using different methods, both the PBE functional and HSE06 hybrid functional were used for N-doped TiO₂, as listed in Table 2. It can be seen that the ener-

Table 2
Energetics comparison of N-doped TiO$_2$ obtained with the PBE and hybrid HSE06 functionals.

TiO$_2$	PBE/eV				HSE06/eV			
	ΔH_1	ΔH_2	ΔH_3	ΔH_4	ΔH_1	ΔH_2	ΔH_3	ΔH_4
Anatase TiO$_2$ (3×3×1)	−0.82	3.11	7.11	4.00	−0.08	3.73	7.26	3.53
Rutile TiO$_2$ (2×2×3)	0.94	2.90	7.20	4.30	2.22	3.30	5.86	2.56

getics did not exhibit a strong dependence on the functional used in this study. Because the HSE06 functional is more time consuming than the PBE, the other anion-doped TiO$_2$ energetics calculations were performed with the standard PBE functional. The results are shown in Fig. 3 and Fig. 4. As the anions do not appear in reaction (3), the values of ΔH_3 do not change for the same system, which are 7.11 and 7.20 eV for anatase and rutile TiO$_2$, respectively. The substitutional anion-doped reaction was strongly endothermic for both anatase and rutile TiO$_2$, but the interstitial anion-doped reaction can be exothermic or slightly endothermic. There existed a large energy barrier for substitutional N-doped TiO$_2$ for both anatase and rutile TiO$_2$, and the value of ΔH_3 was a quite positive number compared with ΔH_1. The larger energy value can explain why substitutional N-doped TiO$_2$ usually requires severe reaction conditions, such as ion implantation and sputtering, or nitridizing TiO$_2$ in N$_2$ or NH$_3$ at high temperatures, whereas interstitial N-doped TiO$_2$ can be prepared via mild wet chemistry reactions. However, this comparison cannot provide insights into
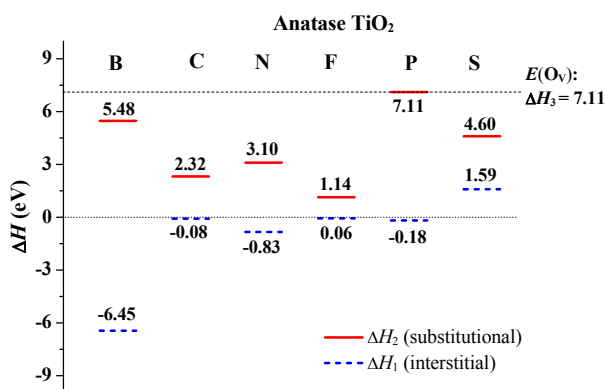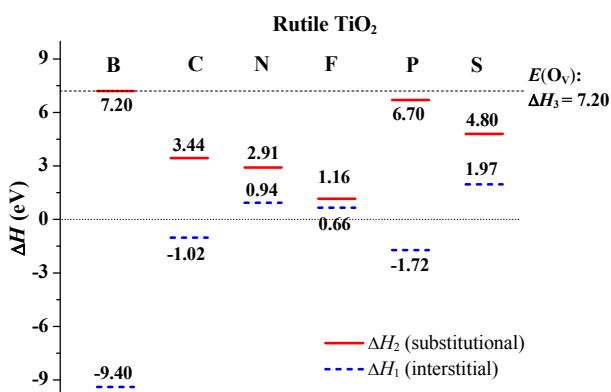
which product is formed at a given severe reaction condition, and the process of how the O atom changed into its final form therefore should be taken into account. In the following part, we used O$_2$ as the final form of the O atom to address this issue. The total energy of O$_2$ was also included in our work, with the energy of a O$_2$ $E(O_2)$ = −9.857 eV and a single O atom $E(O)$ = −1.90 eV. Thus another reaction is O = 0.5O$_2$ + ΔH_5, with the value of ΔH_5 = −3.02 eV. ΔH_5 should be added to ΔH_2, and then compared with ΔH_1. Fig. 3 shows that for B- or P-doped TiO$_2$, interstitial doping was still more favorable than substitutional doping, which means that under severe conditions and with the final form of O, interstitial B- or P-doped TiO$_2$ is still more easily prepared than substitutional B- or P-doped TiO$_2$. N-, C-, or S-doped TiO$_2$ tended to have a similar enthalpy change, while F-doped TiO$_2$ showed the reversed trend. As the value of ΔH_5 depended on the final form of the O atoms, different preparation solutions can lead to different mixtures of interstitial and substitutional doped products. In experimental preparations when severe conditions were provided for N doping of TiO$_2$, there were always two N 1s peaks in the XPS spectra [3,9,12] whereas when the conditions used were mild, there was only one peak [23,24]. From the energetics study, we can identify that with a mild environment, only interstitial N-doped TiO$_2$ is produced, and both types of N-doped TiO$_2$ exist when severe conditions are used.

3.3. CLS study of anion-doped TiO$_2$

3.3.1. CLS study of interstitial and substitutional doping

For the core level of the anion doped into TiO$_2$, the two different types of doping: substitutional and interstitial doping showed two close peaks in the XPS spectra. These two peaks cannot be distinguished just by the experimental data, and the CLS by a DFT study can be used to identify these close peaks. We have found that the most stable location is the interstitial site. Then, we performed a CLS study of the two different doping types with standard DFT for B-, C-, N-, F-, P-, and S-doped TiO$_2$. The results are shown in Fig. 5 and Table 3.

From Fig. 5, we can see that for B-, C-, N-, F-, P-, and S-doped TiO$_2$, there exists a clear difference between substitutional and interstitial doping. Most interstitial anion dopants type had a higher core level binding energy than that of the substitutional dopant, except for F-doped TiO$_2$. For N-doped TiO$_2$, it was
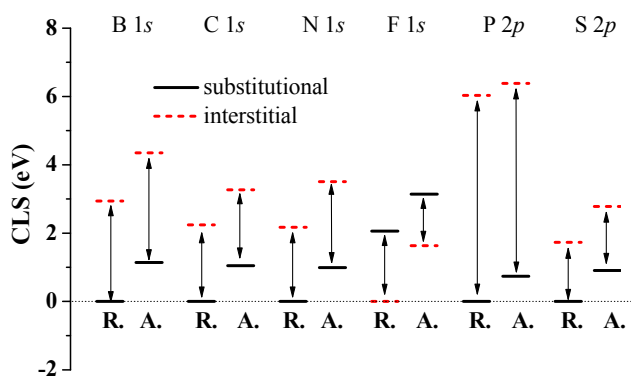
Fig. 3. Comparison of enthalpy change for anion-doped anatase TiO$_2$.

Fig. 4. Comparison of enthalpy change for anion-doped rutile TiO$_2$.

Fig. 5. CLS results of anion-doped anatase TiO$_2$ and rutile TiO$_2$.

Table 3
Calculated B, C, N, and F 1*s* and P and S 2*p* CLSs in anion-doped anatase and rutile TiO₂. The energy references are substitutional rutile (2×2×3) for B, C, N, P, and S and interstitial rutile (2×2×3) for F.

TiO₂		CLS (eV)					
		B 1*s*	C 1*s*	N 1*s*	P 2*p*	S 2*p*	F 1*s*
Anatase TiO₂	interstitial	4.26	3.10	3.38	6.41	2.79	1.47
(3×3×1)	substitutional	1.05	0.88	0.86	0.77	0.92	2.98
Rutile TiO₂	interstitial	2.94	2.24	2.17	6.03	1.73	0
(2×2×3)	substitutional	0	0	0	0	0	2.06

found that the N 1*s* core level binding energy of the interstitial N species was higher than that of the substitutional N species for both N-doped anatase TiO₂ and rutile TiO₂. The CLSs were 2.52 and 2.17 eV for N-doped anatase and rutile TiO₂, respectively. Experimentally, N 1*s* XPS peaks with different binding energies have been observed by XPS for N-doped TiO₂ prepared by different methods. Asahi et al. [3] assigned the N 1*s* peak with a binding energy at 396 eV to substitutional N in N-doped anatase TiO₂ prepared by sputtering a TiO₂ target in a N₂ atomsphere. Chen et al. [32] attributed the N 1*s* peak with a binding energy at 401.3 eV to substitutional N in N-doped anatase TiO₂ prepared by treating TiO₂ with an excess of triethylamine. Diwald et al. [9] prepared N-doped rutile TiO₂(110) by heating in NH₃ and observed two N 1*s* peaks with binding energies at 396.7 and 399.6 eV, which were assigned to substitutional and interstitial N atoms, respectively. Fang et al. [23] assigned the N 1*s* peak with a binding energy at 399.6 eV to interstitial N in N-doped anatase TiO₂ prepared by a wet chemistry method. Comparing the N in TiN with a N 1*s* binding energy at 397 eV [57], it has been generally accepted that the N 1*s* peak with a binding energy at 396–397 eV is from substitutional N in N-doped TiO₂. However, the evidence for the assignment of the N 1*s* peak with a binding energy at 399.6 eV to interstitial N in N-doped TiO₂ is lacking. Our theoretical calculations fully support the assignments: substitutional N in N-doped TiO₂ exhibits N 1*s* binding energy between 396 and 397 eV and interstitial N in N-doped TiO₂ exhibits the N 1*s* binding energy at 399.6 eV. Our results also suggested the assignment of the N 1*s* peak with a binding energy at 401.3 eV to substitutional N in N-doped anatase TiO₂ already made by Chen et al. [32]. Meanwhile, on basis of the calculated enthalpy for the N-doping reaction, it is also reasonable to conclude that treating TiO₂ with an excess of triethylamine that was employed by Chen et al. [32] should not be able to form the substitutional N species.

3.3.2. CLS study of the different anions

We summarized the CLS results of different anion-doped TiO₂ in Fig. 5 and Table 3. Our calculations showed that the E_{CLS} value of anion-doped TiO₂ was positive except for F-doped TiO₂. This means that in the XPS spectra of anion-doped TiO₂, the interstitial doping peak is located higher than that of substitutional doping. The CLS results (Fig. 5) showed that the F atom gave a reverse trend compared with other anions. This can be understood through the Pauli electronegativity of these atoms [56] (Table 1). The electronegativity value of O is larger than those of B, C, N, P, and S, while smaller than that of F. After an O

atom is substituted by an anion, the Ti atoms are closer than with the O atoms, while for interstitial doping, the O atoms are closer than the anion. The difference in the structure between substitutional and interstitial doping is that more nearby O atoms surround the anion in interstitial doping. According to the sequence of the electronegativity [56], there is more electron transfer from O to F in interstitial doping than substitutional doping; while for B-, C-, N-, P-, or S-doping of TiO₂, there is the reverse electron transfer direction, and substitutional doping gets more electrons than interstitial doping. As we know, when more electrons are moved away, the binding energy would be larger. Thus, the B, C, N, P, and S atoms in interstitial doping sites have a higher core level energy than those in substitutional doping sites; and F-doped TiO₂ has a reverse trend. When this conclusion is applied to the XPS spectra, for B-, C-, N-, P-, and S-doped TiO₂, the peak from interstitial doping is higher than that from substitutional doping; and for F-doped TiO₂, that from substitutional doping is higher than interstitial doping.

3.3.3. CLS study between the different phases of TiO₂

We have studied the anion CLS for both the rutile and anatase, as shown in Fig. 5 and Table 3. The results revealed that both anatase and rutile showed the same sequence of the substitutional and interstitial dopant peaks. However, for the same dopant, the core level binding energy of the anion in anatase is a little higher than that in rutile. The probable reason may be that the density of rutile is larger than that of anatase. As the distance between two neighboring atoms is less, the interaction between Ti and the anion is stronger, thus, the anion can accept more electrons in rutile than anatase. As discussed above, when more electrons are lost, the core level binding energy is higher. Therefore, the binding energy of the anion in anatase is higher than in rutile.

4. Conclusions

We have performed comprehensive and improved DFT calculations of anion-doped anatase and rutile TiO₂. The N 1*s* core level binding energy calculations suggested that interstitial N species exhibit a higher N 1*s* binding energy than substitutional N species in N-doped TiO₂. The calculated core level shift between interstitial and substitutional N species agreed well with experimental data, which strongly supports the assignments of the experimental XPS results. Our calculations provide a fundamental understanding of N-doped TiO₂ photocatalysts. We also performed CLS calculations for B-, C-, F-, P-, and S-doped TiO₂ and show that in F-doped TiO₂, the interstitial dopant peak is lower than that of the substitutional dopant. However, for B-, C-, N-, P-, and S-doped TiO₂, the peak of the interstitial dopant is higher than that of the substitutional dopant. The enthalpy calculations demonstrated that the substitutional anion-doped reaction is strongly exothermic for both anatase and rutile TiO₂ due to the intermediate production of oxygen vacancies, whereas the interstitial anion-doped reaction is modestly endothermic. Our calculations suggested that for B, C, N, F, P, and S anion-doped TiO₂, severe experimental conditions are re-

quired for substitutional doping, while for interstitial doping, wet chemistry methods would be enough.

References

[1] Fujishima A, Honda K. *Nature*, 1972, 238: 37
[2] Fujishima A, Rao T N, Tryk D A. *J Photochem Photobiol C*, 2000, 1: 1
[3] Asahi R, Morikawa T, Ohwaki T, Aoki K, Taga Y. *Science*, 2001, 293: 269
[4] Khan S U M, Al-Shahry M, Ingler W B Jr. *Science*, 2002, 297: 2243
[5] Chen X B, Mao S S. *Chem Rev*, 2007, 107: 2891
[6] Lindgren T, Mwabora J M, Avendano E, Jonsson J, Hoel A, Granqvist C G, Lindquist S E. *J Phys Chem B*, 2003, 107: 5709
[7] Mwabora J M, Lindgren T, Avendano E, Jaramillo T F, Lu J, Lindquist S E, Granqvist C G. *J Phys Chem B*, 2004, 108: 20193
[8] Nakano Y, Morikawa T, Ohwaki T, Taga Y. *Appl Phys Lett*, 2005, 86: 132104
[9] Diwald O, Thompson T L, Goralski E G, Walck S D, Yates J T Jr. *J Phys Chem B*, 2004, 108: 52
[10] Batzill M, Morales E H, Diebold U. *Phys Rev Lett*, 2006, 96: 026103
[11] Ghicov A, Macak J M, Tsuchiya H, Kunze J, Haeublein V, Frey L, Schmuki P. *Nano Lett*, 2006, 6: 1080
[12] Irie H, Watanabe Y, Hashimoto K. *J Phys Chem B*, 2003, 107: 5483
[13] Yu J G, Yu J C, Leung M K P, Ho W, Cheng B, Zhao X J, Zhao J C. *J Catal*, 2003, 217: 69
[14] Burda C, Lou Y B, Chen X B, Samia A C S, Stout J, Gole J L. *Nano Lett*, 2003, 3: 1049
[15] Sakthivel S, Janczarek M, Kisch H. *J Phys Chem B*, 2004, 108: 19384
[16] Gole J L, Stout J D, Burda C, Lou Y B, Chen X B. *J Phys Chem B*, 2004, 108: 1230
[17] Wang Z P, Cai W M, Hong X T, Zhao X L, Xu F, Cai C G. *Appl Catal B*, 2005, 57: 223
[18] Li H X, Li J X, Huo Y N. *J Phys Chem B*, 2006, 110: 1559
[19] Livraghi S, Paganini M C, Giamello E, Selloni A, Di Valentin C, Pacchioni G. *J Am Chem Soc*, 2006, 128: 15666
[20] Kisch H, Sakthivel S, Janczarek M, Mitoraj D. *J Phys Chem C*, 2007, 111: 11445
[21] Cong Y, Zhang J L, Chen F, Anpo M. *J Phys Chem C*, 2007, 111: 6976
[22] Wang J W, Zhu W, Zhang Y Q, Liu S X. *J Phys Chem C*, 2007, 111: 1010
[23] Fang J, Wang F, Qian K, Bao H Z, Jiang Z Q, Huang W X. *J Phys Chem C*, 2008, 112: 18150
[24] Huo Y N, Bian Z F, Zhang X Y, Jin Y, Zhu J, Li H X. *J Phys Chem C*, 2008, 112: 6546

[25] Joung S K, Amemiya T, Murabayashi M, Itoh K. *Appl Catal A*, 2006, 312: 20
[26] Liu G, Li F, Chen Z G, Lu G Q, Cheng H M. *J Solid State Chem*, 2006, 179: 331
[27] He F, Ma X F, Li T, Li G X. *Chin J Catal*, 2013, 34: 2263
[28] Mohamed R M, Aazam E. *Chin J Catal*, 2013, 34: 1267
[29] Zhou W Q, Yu C L, Fan Q Z, Wei L F, Chen J C, Yu J C. *Chin J Catal*, 2013, 34: 1250
[30] Liu E Q, Guo X L, Qin L, Shen G D, Wang X D. *Chin J Catal*, 2012, 33: 1665
[31] Serpone N. *J Phys Chem B*, 2006, 110: 24287
[32] Chen X B, Burda C. *J Phys Chem B*, 2004, 108: 15446
[33] Rodriguez J A, Jirsak T, Liu G, Hrbek J, Dvorak J, Maiti A. *J Am Chem Soc*, 2001, 123: 9597
[34] Lu N, Quan X, Li J Y, Chen S, Yu H T, Chen G H. *J Phys Chem C*, 2007, 111: 11836
[35] Zaleska A, Sobczak J W, Grabowska E, Hupka J. *Appl Catal B*, 2008, 78: 92
[36] Finazzi E, Di Valentin C, Pacchioni G. *J Phys Chem C*, 2009, 113: 220
[37] Bettinelli M, Dallacasa V, Falcomer D, Fornasiero P, Gombac V, Montini T, Romano L, Speghini A. *J Hazard Mater*, 2007, 146: 529
[38] Chen D M, Yang D, Wang Q, Jiang Z Y. *Ind Eng Chem Res*, 2006, 45: 4110
[39] Zhao W, Ma W H, Chen C C, Zhao J C, Shuai Z G. *J Am Chem Soc*, 2004, 126: 4782
[40] Moon S C, Mametsuka H, Tabata S, Suzuki E. *Catal Today*, 2000, 58: 125
[41] Czoska A M, Livraghi S, Paganini M C, Giamello E, Di Valentin C, Pacchioni G. *Phys Chem Phys Chem*, 2011, 13: 136
[42] Di Valentin C, Pacchioni G, Onishi H, Kudo A. *Chem Phys Lett*, 2009, 469: 166
[43] Di Valentin C, Finazzi E, Pacchioni G, Selloni A, Livraghi S, Czoska A M, Paganini M C, Giamello E. *Chem Mater*, 2008, 20: 3706
[44] Di Valentin C, Finazzi E, Pacchioni G, Selloni A, Livraghi S, Paganini M C, Giamello E. *Chem Phys*, 2007, 339: 44
[45] Di Valentin C, Pacchioni G, Selloni A, Livraghi S, Giamello E. *J Phys Chem B*, 2005, 109: 11414
[46] Di Valentin C, Pacchioni G, Selloni A. *Chem Mater*, 2005, 17: 6656
[47] Heyd J, Scuseria G E, Ernzerhof M. *J Chem Phys*, 2006, 124: 219906
[48] Heyd J, Scuseria G E. *J Chem Phys*, 2004, 121: 1187
[49] Heyd J, Scuseria G E, Ernzerhof M. *J Chem Phys*, 2003, 118: 8207
[50] Kresse G, Hafner J. *Phys Rev B*, 1993, 48: 13115
[51] Kresse G, Hafner J. *Phys Rev B*, 1994, 49: 14251
[52] Kresse G, Furthmuller J. *Phys Rev B*, 1996, 54: 11169

Graphical Abstract

Chin. J. Catal., 2015, 36: 181–187　　　doi: 10.1016/S1872-2067(14)60165-0

A first principles study of the energetics and core level shifts of anion-doped TiO$_2$ photocatalysts

Wuchen Ding, Weixue Li *
Dalian Institute of Chemical Physics, Chinese Academy of Sciences

Core level shifts in B-, C-, N-, S-, or P-doped TiO$_2$ are such that the energy of an interstitial dopant is higher than that of a substitutional dopant, but for F-doped TiO$_2$, the energy of the substitutional dopant is higher.
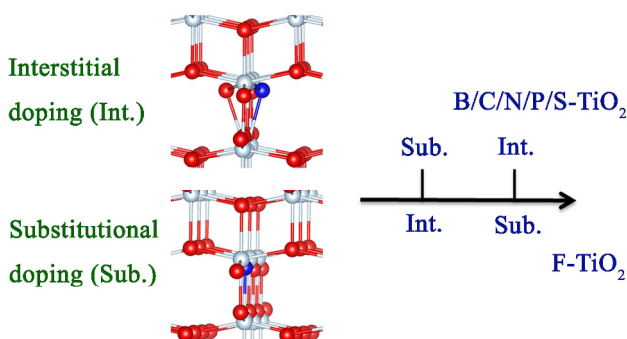
[53] Kresse G, Furthmuller J. *Comput Mater Sci*, 1996, 6: 15

[54] Krukau A V, Vydrov O A, Izmaylov A F, Scuseria G E. *J Chem Phys*, 2006, 125: 224106

[55] Slater J C. *J Chem Phys*, 1964, 41: 3199

[56] Allred A L. *J Inorg Nucl Chem*, 1961, 17: 215

[57] Saha N C, Tompkins H G. *J Appl Phys*, 1992, 72: 3072